

Enhanced in-field critical currents of YBCO second-generation (2G) wire by Dy additions

This article has been downloaded from IOPscience. Please scroll down to see the full text article.

2005 Supercond. Sci. Technol. 18 S405

(<http://iopscience.iop.org/0953-2048/18/12/030>)

View [the table of contents for this issue](#), or go to the [journal homepage](#) for more

Download details:

IP Address: 131.215.225.9

The article was downloaded on 12/10/2010 at 17:38

Please note that [terms and conditions apply](#).

Enhanced in-field critical currents of YBCO second-generation (2G) wire by Dy additions

N Long¹, N Strickland¹, B Chapman¹, N Ross¹, J Xia¹, X Li²,
W Zhang², T Kodenkandath², Y Huang² and M Rupich²

¹ Industrial Research Ltd, PO Box 31-310, Lower Hutt, New Zealand

² American Superconductor Corporation, Westborough, MA 01581, USA

Received 28 July 2005, in final form 21 September 2005

Published 16 November 2005

Online at stacks.iop.org/SUST/18/S405

Abstract

The addition of dysprosium oxide nanoparticles is shown to improve the critical current in perpendicular magnetic fields for second-generation (2G) wire formed by metal–organic deposition (MOD). Typical enhancements in J_c are from 0.17 MA cm^{-2} to over 0.33 MA cm^{-2} at 77 K and $B_{\text{perp}} = 1.5 \text{ T}$. TEM analysis shows that we are introducing $(\text{Y, Dy})_2\text{O}_3$ nanoparticles with dimensions of 10–50 nm. A simple theoretical analysis shows that the maximum pinning effect for additions is expected at excess concentrations of approximately 70% $\text{DyO}_{1.5}$, i.e. for $\text{YBa}_2\text{Cu}_3\text{O}_{7-\delta} + 0.7\text{DyO}_{1.5}$ if the added nanoparticles are randomly dispersed and a strong pinning model is valid. An interesting feature is that the critical current in parallel field is reduced in these samples. We present evidence that shows this may be due to reduced planar defects in the YBCO.

1. Introduction

The development of 2G wire based on YBCO has accelerated greatly in recent years. Progress is focused on making longer, wider and higher I_c tapes [1–4]. A challenge that remains is to maximize the critical current in moderate fields of 1–3 T. In a magnetic field, magnetic flux penetrates into a type II superconductor. When a current flows in the superconductor there is a Lorentz force which will cause a dissipative motion of the vortices unless they are ‘pinned’ in place. A normal phase defect enhances pinning as it is energetically favourable for the vortex core to occupy the same volume as the defect. Many approaches are possible for increasing the density of normal phase defects such as ion irradiation [5], co-deposition of normal phases [6–8], or the introduction of substrate defects [9, 10]. Pinning is optimized when the size of the defects approaches the superconducting coherence length ($\xi_{\text{ab}} \sim 7 \text{ nm}$ for YBCO at 77 K) and when the areal number density of defects is of the order of $2eB_{\text{ext}}/h$, where B_{ext} is the applied magnetic field. In every experimental approach the challenge is to introduce defects uniformly throughout the superconductor which can meet these criteria.

The metal–organic deposition process lends itself naturally to the inclusion of nanoparticles (also called

nanodots) through the spontaneous growth of secondary phases in the YBCO matrix. When excess quantities of rare-earth (RE) ions in the form of a metal–organic complex are added to the precursor solutions these have been found to form dispersions of 10–50 nm sized particles in the fully reacted YBCO. RE ions are chosen as they are chemically inert with respect to the YBCO and any substitution within the YBCO matrix is likely to be benign. MOD is a low-cost process which is vital to successful commercialization of the technology. The additional process steps required to add nanoparticles in this way are minimal.

2. Experimental details

2.1. Sample fabrication

The substrates used are based on the RABiTS process. A cube-textured NiW(5%) alloy substrate is buffered with oxide layers with the structure $\text{CeO}_2/\text{YSZ}/\text{Y}_2\text{O}_3/\text{NiW}$. The oxide layers all have 75 nm thickness and their deposition is described in more detail elsewhere [1]. A trifluoroacetate (TFA) precursor was deposited by spin coating at approximately 2000 rpm on a $1.5 \text{ cm} \times 1 \text{ cm}$ sample for 60 s or by slot die coating on a longer length of substrate. The MOD film was pyrolysed for 1–2 h

at temperatures $<600^\circ\text{C}$ in a humid oxidizing atmosphere to remove most of the organic components, leaving a film with a nominal composition of $0.5\text{Y}_2\text{O}_3\text{-}2\text{BaF}_2\text{-}3\text{CuO}$. This film was then reacted to an epitaxial YBCO film by inserting the film into a furnace at $700\text{-}800^\circ\text{C}$ in a controlled $\text{O}_2\text{-H}_2\text{O}$ environment. The processed YBCO film was capped with $1\text{-}3\ \mu\text{m}$ of Ag by thermal evaporation and then oxygen loaded at $400\text{-}500^\circ\text{C}$. This also establishes good Ag contact to the YBCO.

To form the nanoparticle additions varying amounts of dysprosium precursor were added to the TFA precursor and the concentration and deposition conditions were adjusted if necessary to maintain an approximately constant thickness of YBCO.

2.2. Measurements

Critical currents were determined by transport measurements at $77\ \text{K}$ with a criterion of $1\ \mu\text{V cm}^{-1}$. The samples were patterned to form a bridge $0.5\ \text{cm}$ wide and $1\ \text{cm}$ long. Voltage taps were placed $1\ \text{cm}$ apart. Measurements were made as a function of field angle and field strength of up to $1.5\ \text{T}$ such that the field direction was perpendicular to the current transport direction.

TEM cross-section samples were prepared by mechanically polishing samples to a thickness of $\sim 20\ \mu\text{m}$ and then milling with Ar^+ ions using Gatan's 691 Precision Ion Polishing System (PIPS). TEM work was performed at Victoria University of Wellington using a JOEL 2011 transmission electron microscope which is operated at $200\ \text{kV}$ with a LaB_6 filament.

3. Theory

In the case of strong pinning [11–14], defects act individually and the pinning force density is linear in the density and average pinning force of the defects. The alternative situation is termed collective pinning, where the pinning results from fluctuations in the average pinning force of many weak pins through the material.

The added nanoparticles in our experiments tend to be larger in dimension than the superconducting coherence length ($\sim 10\ \text{nm}$) and we assume that they are acting as strong pinning centres. To estimate the optimal amount of additional material we make a number of simplifying assumptions and apply the results from studies of the clustering properties of Poisson distributed overlapping spheres [15]. The maximum pinning will of course depend on the interaction between all defects in the material, including defects native to the YBCO; however, if we assume the added nanoparticles dominate, this calculation gives a useful guide to the experiments.

We assume that the added normal phase exists as spheres of equal size which are Poisson distributed and which can overlap. That is, in this model larger defects or clusters are formed from k overlapping smaller spheres. In the language of Quintanilla and Torquato these are termed k -mers (a cluster of k spheres). To maximize pinning we want to find what volume fraction of added spheres gives us the maximum density of clusters; we call this n_{max} . We assume that each cluster or k -mer can pin one vortex with equal pinning strength.

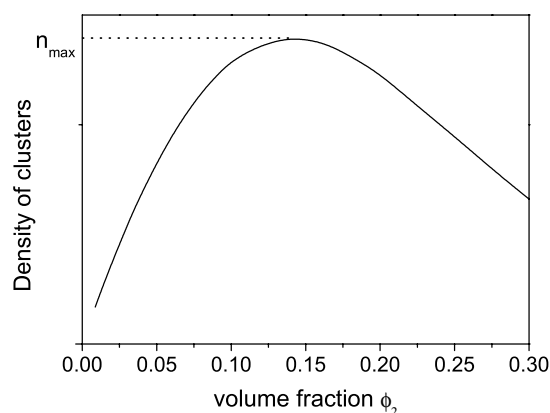


Figure 1. Estimate of total density of clusters versus volume fraction of overlapping spheres using the model of Quintanilla and Torquato [15].

Consider a virgin material to which spheres are added. At low density the majority of particles will be monomers (1-mers) and as the density increases the number of k -mers increases for all k . However, as further spheres are added there is a particular volume fraction for each k at which the number of k -mers starts to decrease. For example, at a particular density it is more likely that an added sphere will result in an existing monomer being overlapped to form a dimer (2-mer) than result in an additional monomer. To estimate the volume fraction for n_{max} we sum the n_k given by Quintanilla and Torquato for $k = 1\text{-}4$. The error in neglecting higher k is not significant [15]. In figure 1 we plot the total density of clusters versus the volume fraction of the added material.

Figure 1 shows that a maximum occurs for a volume fraction of approximately $\phi_2 = 0.14$. An important point is that this is independent of the size of the added spheres in the model. That is, we will always obtain the maximum number of clusters by having a volume fraction of 0.14 additional material, independent of the average size of the clusters. This should hold for our added nanodots. Irrespective of the size of the nanodots the correct volume fraction is 0.14.

We can now make an estimate of the amount of material that will maximize pinning. Using the known unit cell volumes for YBCO and Dy_2O_3 we can calculate that the volume fraction of 0.14 occurs for the composition $\text{YBa}_2\text{Cu}_3\text{O}_{7-\delta} + 0.7\text{DyO}_{1.5}$ assuming that all the added Dy_2O_3 is contained in normal phase precipitates. The proviso remains that to form an effective pinning site a cluster needs to be at least of order of the coherence length, $\xi \sim 10\ \text{nm}$. If a significant amount of added material exists in nanoparticles with dimensions smaller than $10\ \text{nm}$ then the maximum pinning may occur for higher volume fractions. It is also possible in this case that the strong pinning model is not valid at all.

4. Results

4.1. Low Dy concentration

We show the results from two datasets. The first set of samples with cation ratios $\text{Y:}2\text{Ba:}3\text{Cu:}x\text{Dy}$ with $x = 0\text{-}0.5$ was made by slot die coating and a continuous decomposition

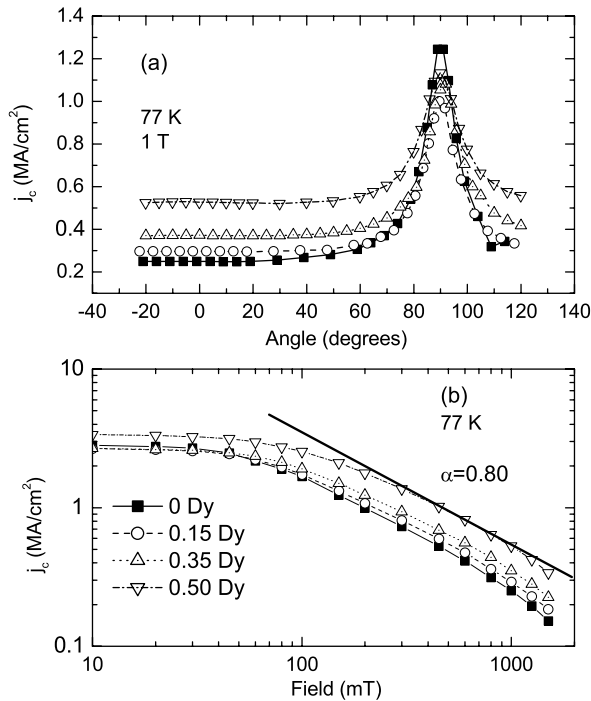


Figure 2. (a) Field angle and (b) field dependence of the critical current density films with cation ratios Y:2Ba:3Cu:xDy with $x = 0, 0.15, 0.25, 0.35, 0.50$.

process. The second set of samples with compositions $x = 0, 0.75, 0.85$ and 1.00 was made using spin coating and a static decomposition.

The results show a monotonic increase in critical current in field perpendicular to the tape plane (we subsequently refer to this as ‘perpendicular field’), with increasing Dy concentration as shown in figures 2(a) and (b). At angles away from the peak where the field is parallel to the plane of the tape (referred to subsequently as ‘parallel field’) the Dy samples have clearly improved critical currents and the critical current has a flat profile. There is no perpendicular field peak to indicate the presence of c -axis correlated defects. All samples have slightly lower critical current in parallel field than the sample with no Dy addition.

Interestingly the $x = 0.50$ Dy sample also shows an increase in the self-field I_c . We do not have any explanation for why this should have occurred. A fit to a general field dependence $I_c \sim B^{-\alpha}$ gives $\alpha = 0.80$ in the region $B = 0.1$ – 1 T. This is a larger exponent than expected if the sample is in a pure strong pinning regime [11].

4.2. High Dy concentration

Further increases in the in-field critical current are possible with higher Dy content. There are small differences between the samples critical currents in perpendicular field with the maximum J_c for the $x = 1.00$ Dy sample. There is a small hint of a peak in J_c in the perpendicular field. For all Dy concentrations in this batch of samples there is a decrease in the parallel field J_c compared with pure YBCO as shown in figure 3. This is much stronger at 1.5 T than at 1 T. There is also some variation in self-field J_c of unknown origin. The

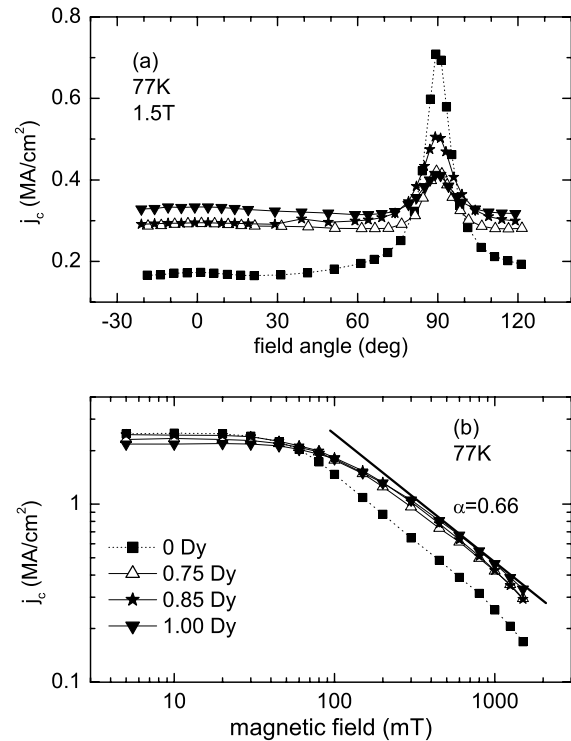


Figure 3. (a) Field angle and (b) field dependence of the critical current density for films with cation ratios Y:2Ba:3Cu:xDy with $x = 0, 0.50, 0.75, 0.85$ and 1.00 .

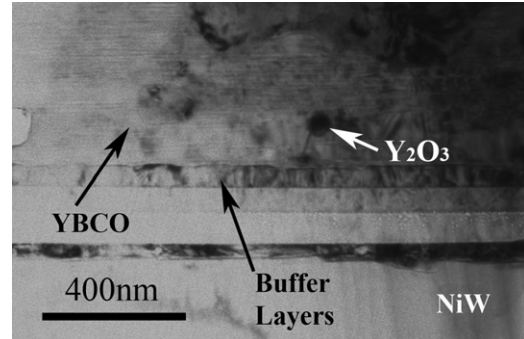


Figure 4. TEM image of standard YBCO material. In the YBCO can be seen a very high density of a - b plane stacking faults. Some Y₂O₃ inclusions of size about 20 nm can also be observed.

field dependence exponent $\alpha = 0.66$, which is comparable to the value of 0.625 predicted by Ovchinnikov and Ivlev for strong pinning [11].

With concentrations higher than $x = 0.50$ the precursor viscosity changes and adjustments have to be made in precursor concentration to ensure a constant thickness. It may be that higher concentrations require further process changes to optimize performance.

4.3. Transmission electron microscopy

A TEM cross-section was prepared from a standard YBCO sample. The microstructure is shown in figure 4. The thickness of the YBCO layer is about 800–900 nm. We commonly

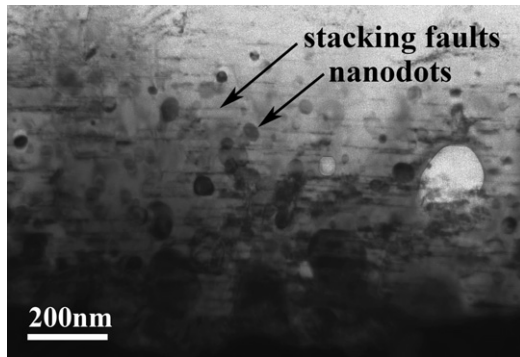


Figure 5. TEM image of Y:2Ba:3Cu:0.5Dy sample. The nanodots have a composition of $(Y, Dy)_2O_3$. Stacking faults are visible at a much lower density than in the undoped YBCO. The nanodot inclusions do not disturb the epitaxy of the YBCO.

observe native defects such as voids and secondary phase particles in the size range 10–50 nm. A very high density of stacking faults was also observed in the a – b plane. Further study of these stacking faults will be performed by high-resolution TEM in the near future.

A Y:2Ba:3Cu:0.7Dy sample was also examined by TEM. Figure 5 shows TEM images of this material. The thickness of YBCO in this sample is about 1.1 μ m. The material contains a similar density of voids to the YBCO. The density of nanoparticles observed in this material is much higher than the standard YBCO material. The size of these particles is in the range 10–50 nm. EDS spectra indicate these particles mainly contain Y and Dy in approximately similar amounts; that is, we are forming $(Y, Dy)_2O_3$ nanoparticles. The stacking faults in the a – b plane were also observed in this material but at a much lower density than for the standard YBCO.

5. Discussion and conclusions

The addition of a dysprosium oxide precursor to the YBCO MOD precursor has proven to be a convenient way to introduce additional pinning centres. A simple theoretical analysis suggests that if the additional material is distributed randomly then the maximum number of pinning sites are created with a cation composition of Y:2Ba:3Cu:0.7Dy. This is broadly consistent with the observed results where we show that the critical current in perpendicular field can be increased with additions of $x = 0.70$ – 1.00 .

This is not the case for the critical current in parallel field. In this instance Dy additions have the effect of always decreasing performance. We hypothesize that this is because

the parallel field performance is dominated by the density of a – b plane defects. From our TEM observations the undoped YBCO has a high density of a – b plane stacking faults. With Dy additions the stacking fault density is greatly reduced. To maintain the parallel field performance we will have to determine how to retain the density of stacking faults while adding RE nanoparticles.

The other requirement for optimized pinning is to maximize the areal density of the pinning centres. To do this we need to control the size of the RE nanodots. We plan to investigate the effect of small changes in process conditions to see whether this can change the average size or the size distribution of the nanodots. Investigation of other RE additions will also focus on whether the size of the nanodots is optimum.

Acknowledgments

We thank D Krouse and G V M Williams for discussions. This work is in part supported by the New Zealand Foundation for Research Science and Technology, contract C08X0407.

References

- [1] Shoop U *et al* 2005 *IEEE Trans. Appl. Supercond.* **15** 2611
- [2] Selvamanickam V *et al* 2005 *IEEE Trans. Appl. Supercond.* **15** 2596
- [3] Iijima Y, Kakimoto K, Sutoh Y, Ajimura S and Saitoh T 2005 *IEEE Trans. Appl. Supercond.* **15** 2590
- [4] Prusseit W, Sigl G, Nemetschek R, Hoffmann C, Hanke J, Lumkemann A and Kinder H 2005 *IEEE Trans. Appl. Supercond.* **15** 2608
- [5] Civale L 1997 *Supercond. Sci. Technol.* **10** A11
- [6] Campbell T A, Haugan T J, Maartense I, Murphys J, Brunke L and Barnes P 2005 *Physica C* **423** 1 (pld yttria particles)
- [7] Haugan T, Barnes P N, Wheeler R, Meisenkothen F and Sumption M 2004 *Nature* **430** 867
- [8] MacManus-Driscoll J L, Foltyn S R, Jia Q X, Wang H, Serquis A, Civale L, Maiorov B, Hawley M E, Maley M P and Peterson D E 2004 *Nat. Mater.* **3** 439
- [9] Albrecht J, Leonhardt S, Habermeier H-U, Brück S, Spolenak R and Kronmüller H 2004 *Physica C* **404** 18
- [10] Nie J C, Yamasaki H, Yamada H, Nakagawa Y, Develos-Bagarinao K and Mawatari Y 2004 *Supercond. Sci. Technol.* **17** 845
- [11] Ovchinnikov Yu N and Ivlev B I 1991 *Phys. Rev. B* **43** 8024
- [12] Matsushita T 2000 *Supercond. Sci. Technol.* **13** 730
- [13] Blatter G, Feigel'man M V, Geshkenbein V B, Larkin A I and Vinokur V M 1994 *Rev. Mod. Phys.* **66** 1125
- [14] Blatter G, Geshkenbein V B and Koopmann J A G 2004 *Phys. Rev. Lett.* **92** 067009
- [15] Quintanilla J and Torquato S 1996 *Phys. Rev. E* **54** 5331